''Bare'' single-particle energies in ^{56}Ni

L. Trache,[1,*] A. Kolomiets,[1] S. Shlomo,[1,2] K. Heyde,[3] H. Dejbakhsh,[1] C. A. Gagliardi,[1] R. E. Tribble,[1] X. G. Zhou,[1] V. E. Iacob,[4] and A. M. Oros[5,*]

[1]*Cyclotron Institute, Texas A&M University, College Station, Texas 77843*

[2]*The Niels Bohr Institute, 17 Blegdamsvej, DK-2100 Copenhagen, Denmark*

[3]*Institute for Theoretical Physics, University of Gent, B-9000 Gent, Belgium*

[4]*Institute of Atomic Physics, Bucharest-Magurele, P.O. Box MG-6, Romania*

[5]*Institute für Kernphysik der Universität zu Köln, Zülpicher Strasse 77, D-50937 Köln, Germany*

(Received 15 July 1996)

The structure of the low-lying levels in the mirror nuclei ^{57}Ni and ^{57}Cu is described within the extended unified model. The problem of single-particle energies in ^{56}Ni is treated in detail. ''Bare'' single-particle energies are extracted from existing experimental data for the energy levels in ^{57}Ni and ^{57}Cu by carefully considering the influence of the coupling to excitations of the core. Important contributions arise, influencing especially the results on the spin-orbit splitting. The differences between the Coulomb energy shifts of various orbitals in ^{56}Ni are discussed and compared with those resulting from Hartree-Fock calculations carried out using a broad range of Skyrme interactions. The parameters of the Woods-Saxon potential reproducing these neutron ''bare'' single-particle energies and the charge root-mean-square radius of ^{56}Ni are extracted. It is demonstrated that the contributions associated with the Thomas-Ehrman effect and the electromagnetic spin-orbit interaction are important and large enough to account for the differences between the Coulomb energy shifts of the single-particle levels in ^{56}Ni. [S0556-2813(96)03711-9]

PACS number(s): 21.60.Cs, 21.10.Sf, 21.10.Pc, 27.40.+z

I. INTRODUCTION

The mirror nuclei ^{57}Ni and ^{57}Cu are one neutron and one proton, respectively, above the doubly closed shell core ^{56}Ni. Their lowest excited states are in first order approximation obtained by promoting the odd nucleon in the available orbitals above the doubly magic core $N=Z=28$, $2p_{3/2}$, $2p_{1/2}$, $1f_{5/2}$, and $1g_{9/2}$, and/or by exciting collective states of the even-even core. In particular the first excited state of ^{56}Ni (2^+) at $E^*=2701$ keV has the features of a quadrupole vibration and is at an energy comparable with the single-particle excitations. Consequently the residual particle-core interaction leads to configuration mixing which affects the purity of the expected single-particle states in an important way.

Data on the low-lying states of ^{57}Ni have been known for some time [1]. However, more precise information about the structure of ^{57}Cu has only become available recently from the experimental studies of its decay and of its low-lying excited states in the $p(^{58}\mathrm{Ni},^{57}\mathrm{Cu})2n$ experiments carried out at the Momentum Achromat Recoil Separator (MARS) of the Texas A&M University [2,3]. In Sec. II, we provide a description of the lowest excited states of the mirror nuclei ^{57}Ni and ^{57}Cu using a version of the extended unified model (EUM) [4] that carefully takes into account the influence of the particle-vibration coupling [5] on the single-particle states. In Sec. III we compare these extracted ''bare'' single-particle energies in ^{56}Ni with those resulting from mean-field calculations of Skyrme Hartree-Fock type. The parameters of the Woods-Saxon potential reproducing these single-particle energies are determined. It is shown that in order to reproduce the differences between the Coulomb energy shifts of the $2p$ and $1f$ orbitals, the contributions associated with the Thomas-Ehrman effect and the electromagnetic spin-orbit interaction must be taken into account. Section IV summarizes the conclusions.

II. ''BARE'' SINGLE-PARTICLE ENERGIES EXTRACTED FROM EXPERIMENTAL DATA

In the present part of the paper we aim at extracting the ''bare'' single-particle states and their energies in the doubly magic nucleus $^{56}_{28}\mathrm{Ni}_{28}$. In many cases the experimental single-particle energies in atomic nuclei are taken as the energy of the first state with the appropriate spin and parity in the spectra of odd-mass nuclei consisting of one neutron (or one proton) outside a closed shell, provided it is experimentally proved that the state has good single-particle character. While in many cases this is a good choice, it is certainly only an approximation. There is always a residual interaction between the outermost particle and the low-lying collective states of the core that changes its energy. In order to extract the bare single-particle energies for comparison with those predicted by mean-field calculations, one has to single out, as well as possible, the contribution of the particle-core interaction and correct for it. This interaction is best known in the case of nuclei with one particle (hole) outside a closed shell, where a weak-coupling picture works rather well, as is the case for ^{57}Ni and ^{57}Cu. Here, we undertake a detailed study of the lowest states in ^{57}Ni for which substantial experimental data exist. We check the model used and adjust the necessary parameters. Then we extend it to ^{57}Cu, where experimental data are scarce.

There is much experimental evidence in nuclei in the re-

[*]On leave from Institute of Atomic Physics, Bucharest, Romania.

gions of $Z=82$, $N=82$, and $Z=50$ that the lowest states in odd-mass nuclei with one particle outside a closed shell can be described as consisting of essentially three types of excitations (see, e.g., [6,7] and references therein): (i) single-particle orbitals from the open shell coupled to the ground state of the core nucleus, (ii) single-particle states coupled to the excited states of the core nucleus, and (iii) hole states in the orbitals of the last filled shell coupled to the $N+2$ (or $Z+2$) core (2p-1h) [two-particle–one-hole states].

We show briefly that this is valid in nuclei around ^{56}Ni as well. The orbitals in the $N=3$ shell are $2p_{3/2}$, $1f_{5/2}$, and $2p_{1/2}$. It is known from the spin of the ground states of ^{57}Ni and ^{57}Cu that the lowest orbital in the $N=3$ shell is $2p_{3/2}$ [1]. The first and second excited states in ^{57}Ni at $E^*=0.768$ MeV, $J^\pi=5/2^-$ and $E^*=1.113$ MeV, $J^\pi=1/2^-$ have good single-particle character [2] and correspond to the next two orbitals. A quick look higher into the energy spectrum shows a group of three levels of negative parity and spins $J^\pi=5/2^-$, $7/2^-$, and $3/2^-$ around the energy of the first excited state in the core at $E(2_1^+)=2701$ keV with half-lives $T_{1/2}=$ 31, 47, and 12 fs, respectively. These are comparable with the half-life of the first 2^+ state of the ^{56}Ni core, $T_{1/2}=33\pm7$ fs, which can be inferred from the measured $B(E2;0^+\rightarrow2^+)=600\pm120$ $e^2\,\mathrm{fm}^4$ [8]. These facts suggest $(2^+\otimes2p_{3/2})$ configurations of the type (ii) discussed above for these three states. The value of the reduced transition probability $B(E2;0\rightarrow2_1^+)=$ 9.4 Weisskopf units (W.u.) is typical for vibrational states and justifies the approach adopted for the core state. Furthermore, the yrast cascade $15/2^-$ ($E^*=5.318$ MeV) $\rightarrow11/2^-$(3.865 MeV)$\rightarrow7/2^-$(2.577 MeV)$\rightarrow3/2^-$(g.s.) in ^{57}Ni follows closely the yrast cascade 6^+(5.316 MeV) $\rightarrow4^+$(3.923 MeV)$\rightarrow2^+$(2.701 MeV)$\rightarrow0^+$(g.s.) in the core nucleus ^{56}Ni, which implies that these states appear from the maximally aligned coupling of the $2p_{3/2}$ orbital to the corresponding excitations of the core. Configurations of the type (iii) are expected to appear above an excitation energy $E(2\text{p-1h})\simeq S_n(^{56}\text{Ni})-S_n(^{58}\text{Ni})=$ 4.424 MeV. The lowest lying of them should be a hole in the $1f_{7/2}$ orbital coupled to the $N=30$ core ^{58}Ni. Indeed, in one-neutron pickup experiments on ^{58}Ni there is one $J^\pi=7/2^-$ state at $E^*=5.235$ MeV [1] which has a considerably larger spectroscopic factor than any neighboring state.

We attempt the description of the low-lying excited states of the mirror nuclei ^{57}Ni and ^{57}Cu using a version of the extended unified model [4] which properly considers the above-mentioned types of configurations and their coupling. The Hamiltonian treats the single-particle and the vibrational excitations of the core as well as the interaction between the various types of degrees of freedom:

$$H=H_{\text{s.p.}}+H_{\text{core}}^{\text{vib}}+H_{\text{PVC}}, \tag{1}$$

where

$$H_{\text{s.p.}}=\Sigma_\alpha\varepsilon_\alpha(a_\alpha^\dagger a_\alpha)$$

$$\text{and}\quad H_{\text{core}}=\Sigma_\lambda\hbar\omega_\lambda\left[(b_\lambda^\dagger b_\lambda)+\frac{2\lambda+1}{2}\right], \tag{2}$$

$a^\dagger$ (a) and $b^\dagger$ (b) are the fermion and the boson creation (annihilation) operators, respectively, and $\epsilon_\alpha(\hbar\omega_\lambda)$ are the single-particle (λ-phonon) energies.

The model takes into account, in principle, two cores (in our case ^{56}Ni and ^{58}Ni) and the coupling between the odd nucleon and the excitations of the core via a particle-vibration coupling (PVC) Hamiltonian [5] in each subspace:

$$H_{\text{PVC}}=-\sum_\lambda k(r)\sum_\mu Y_{\lambda\mu}^*\alpha_{\lambda\mu}. \tag{3}$$

The excitations of the spherical cores were considered harmonic vibrations of quadrupole and octupole type. The procedure follows closely that used in the recent study of the single-particle energies in $N=83$ nuclei [9].

In the earlier versions of the EUM [4] the radial dependence of the PVC Hamiltonian was dropped by introducing the dimensionless parameters ξ_λ:

$$H_{\text{PVC}}=-\sum_{\lambda=2,3}\xi_\lambda\hbar\omega_\lambda\left(\frac{\pi}{2\lambda+1}\right)^{1/2}\times\sum_\mu[b_{\lambda\mu}^\dagger+(-)^\mu b_{\lambda-\mu}]Y_{\lambda\mu}^*, \tag{4}$$

where

$$\xi_\lambda=\frac{\beta_\lambda}{\sqrt{\pi}}\frac{\langle k_\lambda(r)\rangle}{\hbar\omega_\lambda}. \tag{5}$$

Above, $\alpha_{\lambda\mu}$ denote the collective coordinates for the surface vibrations, which can be expressed in terms of bosonic creation and annihilation operators $b_{\lambda\mu}^\dagger$ and $b_{\lambda\mu}$. The parameter β_λ is the amplitude of the zero-point oscillations in the ground state of the core (or dynamic deformation) extracted from inelastic scattering or from the reduced transition probability $B(E\lambda;0\rightarrow\lambda)$ and the average radial matrix element is $\langle k(r)\rangle=40$–50 MeV [5]. One difference from the procedure outlined in Ref. [4] is that in the present calculations we consider the full radial dependence of H_{PVC} (we shall see later that this is important). The radial form factor

$$\xi_\lambda(r)=-\frac{\beta_\lambda}{\sqrt{\pi}}\frac{K_\lambda r^\lambda}{\hbar\omega_\lambda} \tag{6}$$

and harmonic oscillator radial wave functions were used to calculate the radial part of the matrix elements. In practice the radial matrix elements $\langle n_1l_1|r^\lambda|n_2l_2\rangle$ were divided by the average of the radial integrals occurring between all the single-particle orbitals considered. This way we ensure that we can keep the parametrization of Eq. (4) and the new dimensionless parameters ξ_λ can be directly compared with those extracted in earlier calculations where the radial dependence was averaged out. The detailed calculations showed that the ^{58}Ni core and the octupole degree of freedom do not contribute significantly, if at all. They will not be discussed in what follows, even though they were always included in the numerical calculations with proper care.

To find the model parameters we made a detailed study of ^{57}Ni. Its lowest excited states arise from the mixing of the

single-particle neutron orbitals $2p_{3/2}$, $2p_{1/2}$, and $1f_{5/2}$ with the quadrupole multiplet of the ground state orbital $(2^+\otimes 2p_{3/2})1/2^-,3/2^-,5/2^-,7/2^-$. In the calculations we took the energy of the quadrupole phonon as the energy of the 2_1^+ state in the core ^{56}Ni (2701 keV). The splitting of the three states ($5/2^-,7/2^-$, and $3/2^-$) known experimentally to be around $E^*=2701$ keV is determined by the interaction between the quadrupole moment of the core state and that of the single-particle state. This is the diagonal part of the particle-vibration coupling term in the Hamiltonian and contributes with an energy shift given by [10]

$$\Delta E((Lj)J)=\kappa_2\langle L\|Q\|L\rangle\langle j\|q\|j\rangle(-)^{j+L+J}\begin{Bmatrix} L & j & J \\ j & L & 2 \end{Bmatrix}. \tag{7}$$

To reproduce the observed spin order and the energy splitting for the quadrupole multiplet, a value $Q_m(2_1^+)=16$ fm^2 for the isoscalar (mass) quadrupole moment of the core state is needed. The quadrupole moment of the single-particle state was calculated to be $q(2p_{3/2})=-8.20$ fm^2 using the radial wave functions in the appropriate Woods-Saxon potential.

The absence of spectroscopic factor data from transfer reactions did not allow an easy fit of the coupling strength ξ_2. For the strength of the quadrupole coupling we used two approaches. In the first one it was fixed using the recently measured dynamic deformation of the quadrupole phonon state: $\beta_\lambda=0.173(17)$ [8]. A value $\xi_2=1.44(14)$ was obtained using Eq. (5) and the recommended value $\langle k(r)\rangle=40$ MeV [5] for the radial matrix element. In this case we used the energies of the quadrupole multiplet members to fit the quadrupole moment of the phonon $Q(2_1^+)$. By fitting the position of the $5/2_1^-$ and $1/2_1^-$ states, we obtained the energies of the $\nu 1f_{5/2}$ and $\nu 2p_{1/2}$ single-particle states relative to that of the ground state orbital $\nu 2p_{3/2}$. The 10% uncertainty in the coupling strength leads to uncertainties of about 15 keV in the position of the $1f_{5/2}$ orbital and 80 keV in the position of the $2p_{1/2}$ orbital.

In the second approach we fitted the strength ξ_2 noting that the quadrupole-quadrupole interaction [Eq. (7)] does not affect the position of the $(2^+\otimes 2p_{3/2})3/2^-$ state. Therefore, its shift from the unperturbed value $E(2^+)=2701$ keV is entirely due to the mixing with other configurations, primarily with the ground state orbital $2p_{3/2}$. Adjusting it to reproduce the energy of the $J^\pi=3/2_2^-$ state at $E^*=3007$ keV, we obtain a value $\xi_2=1.39$, which is consistent with the above estimate and is similar to those obtained for the $N=83$ region. The fit of the energies of the lowest six excited states is slightly better in this case; we shall use these values in our final conclusions.

Using the above coupling Hamiltonian we calculated the energies and the wave functions for the states in ^{57}Ni. In all cases the basis contained core states with up to three quadrupole phonons, two octupole phonons, and states with $(2^+\otimes 3^-)R$ configurations in order to minimize the effects of the truncation of the basis. We checked that extending the basis up to $E^*=9$ MeV and introducing the intruder $1g_{9/2}$ orbital at $\varepsilon(1g_{9/2})=7.0$ MeV had little or no effect for the lower states. The parameters used in the calculations are presented in Table I. Only the relevant parameters for the quadrupole coupling and the first core are presented. The results for both nuclei are summarized and compared with the experimental data in Table II. The calculated and experimental spectra for ^{57}Ni are compared in Fig. 1. We notice that the $J^\pi=1/2^-$ member of the quadrupole multiplet is pushed up well above the yrast line by a combined effect of the diagonal quadrupole-quadrupole interaction and by the mixing with the single-particle orbital $2p_{1/2}$. This must be the main reason it has not been observed experimentally. The second $7/2^-$ state included in the figure is mainly of $(2^+\otimes 1f_{5/2})7/2^-$ character. With the wave functions obtained

TABLE I. The parameters used in the EUM calculations for ^{57}Ni and ^{57}Cu.

Parameter	^{57}Ni	^{57}Cu
$\hbar\omega_2$ [MeV]	2.701	2.701
ξ_2	1.39	1.39
$Q(2_1^+)$ [fm^2]	+16	+16
$\varepsilon(2p_{3/2})$ [MeV]	0	0
$\varepsilon(1f_{5/2})$ [MeV]	0.830	1.120
$\varepsilon(2p_{1/2})$ [MeV]	1.880	1.820
$\varepsilon(1g_{9/2})$ [MeV]	7.0	7.0

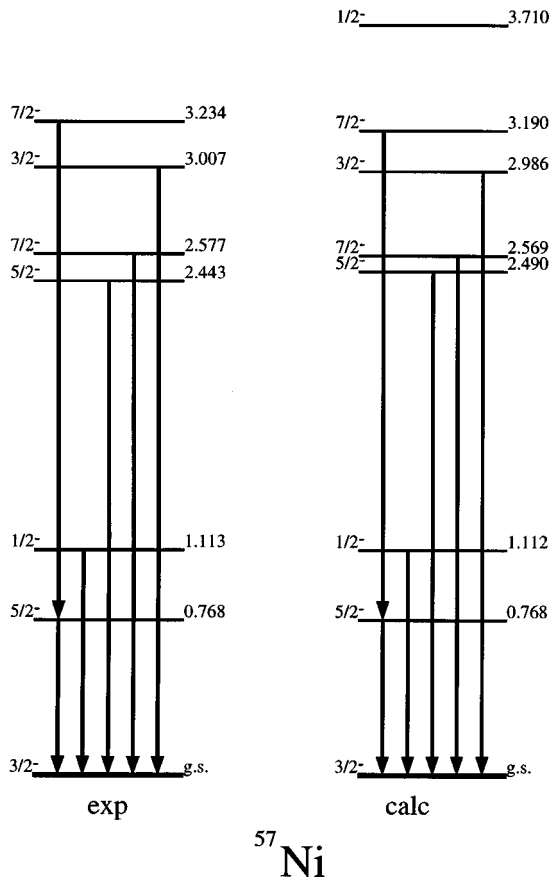

FIG. 1. Comparison between the experimental and calculated level schemes for ^{57}Ni. The energies are in MeV. The results shown are obtained with the coupling constant $\xi_2=1.39$. Data are from Ref. [1].

TABLE II. Comparison between experimental and calculated properties of the lowest-lying levels of ^{57}Ni and ^{57}Cu. Data are from Refs. [1–3]. All energies are in MeV and half-lives in fs.

^{57}Ni								^{57}Cu				
Expt.				Calc.				Expt.		Calc.		Dominant configuration
E^*	J^π	$T_{1/2}$	B(GT)	E^*	J^π	$T_{1/2}$	B(GT)	E^*	J^π	E^*	J^π	
0	$3/2^-$	–	0.204(12)	0	$3/2^-$	–	0.223	0	$3/2^-$	0	$3/2^-$	$2p_{3/2}$
0.768	$5/2^-$	3.2(4)e3	0.014(1)	0.768	$5/2^-$	183.e3	0.0001	1.028	$(5/2^-)$	1.028	$5/2^-$	$1f_{5/2}$
1.113	$1/2^-$	106(23)	0.164(12)	1.112	$1/2^-$	37	0.156	1.106	$(1/2^-)$	1.106	$1/2^-$	$2p_{1/2}$
2.443	$5/2^-$	31(5)	0.009(2)	2.490	$5/2^-$	25	0.0009	2.398	$(5/2^-)$	2.514	$5/2^-$	$(2^+\otimes p_{3/2})5/2^-$
2.577	$7/2^-$	47(6)	0	2.569	$7/2^-$	37	0	2.520	$(7/2^-)$	2.613	$7/2^-$	$(2^+\otimes p_{3/2})7/2^-$
3.007	$3/2^-$	12(4)	0.032	2.986	$3/2^-$	10	0.0016			3.012	$3/2^-$	$(2^+\otimes p_{3/2})3/2^-$
3.234	$7/2^-$			3.190	$7/2^-$	31				3.483	$7/2^-$	$(2^+\otimes f_{5/2})7/2^-$
				3.710	$1/2^-$	34				3.748	$1/2^-$	$(2^+\otimes p_{3/2})1/2^-$

we calculate electromagnetic transition rates by taking the collective $E2$ contribution taken from the core nucleus ^{56}Ni, and using the rather arbitrary, but usual, choice for the effective charge $e_{\rm eff}=0.6e$ and gyromagnetic factors $g_s^{\rm eff}=0.6g_s^{\rm bare}$ for the single-particle part and $g_{\rm coll}=Z/A$ for the collective part. We obtain for ^{57}Ni the decay patterns shown in Fig. 1 and the half-lives shown in the seventh column of Table II. They compare well with those measured. The only notable discrepancy is for the transition $5/2_1^-\rightarrow 3/2_1^-$ (mainly $1f_{5/2}$ and $2p_{3/2}$, respectively) for which the experiment found a larger than expected $M1$ transition probability [1]. The $M1$ transition is forbidden between the main components of the wave functions. Therefore the calculated $M1$ contribution in this case comes entirely from second order to second order terms in the wave functions and is more difficult to evaluate in a reliable way. The magnetic moment for the ground state is calculated to be $\mu_{\rm calc}(g.s.)=-0.93\mu_N$ in good agreement with the measured one $|\mu_{\rm expt}(g.s.)|=0.88(6)\mu_N$ [1]. A further test of the wave functions was to calculate the Gamow-Teller B(GT) matrix elements between the ground state of ^{57}Cu and the low-lying states in ^{57}Ni. Taking into account a quenching of 40% in the Gamow-Teller single-particle strength, we obtain the values listed in the eighth column of Table II. They compare well with the experimental values taken from Ref. [2].

The good agreement of the calculated energies, B(GT) values, gamma-decay half-lives, and magnetic moment of the ground state with the experimental data shows the validity of the entire approach. We stress that the agreement for the B(GT), lifetimes, and magnetic moment was obtained without any attempt to fit the effective Gamow-Teller strength, the effective charges, or the effective gyromagnetic factors, but rather using some reasonable values.

By reproducing the position of the experimental $5/2_1^-$ and $1/2_1^-$ states we find the energy of the ''bare'' single-particle states relative to the $\nu 2p_{3/2}$ orbital:

$$\epsilon(\nu 1f_{5/2})-\epsilon(\nu 2p_{3/2})=0.830\ \text{MeV}, \tag{8}$$

$$\epsilon(\nu 2p_{1/2})-\epsilon(\nu 2p_{3/2})=1.880\ \text{MeV}. \tag{9}$$

We notice that they differ from what we obtain if we neglect the particle-vibration coupling and take for the single-particle energies those of the first states of the appropriate spin and parity. The correction is considerably larger for the $2p_{1/2}$ orbital, due to a larger quadrupole coupling with the ground state orbital and the proximity of the unperturbed state to the quadrupole multiplet. The large difference in the coupling of the $(2^+\otimes 2p_{3/2})$ multiplet to the $1f_{5/2}$ and $2p_{1/2}$ single-particle orbitals is mainly due to the corresponding large difference between the radial integrals $\langle 1f_{5/2}|r^2|2p_{3/2}\rangle$ and $\langle 2p_{1/2}|r^2|2p_{3/2}\rangle$ (different number of nodes of the radial wave function in the first case, but identical in the second). The correction due to taking into account the residual particle-core interaction is especially important for the spin-orbit splitting. The spin-orbit splitting of the $2p$ orbitals changes from 1.11 MeV to 1.88 MeV, a 70% change.

We can extract the corresponding proton single-particle energies using exactly the same procedure, the same value for the coupling strength and for the quadrupole moment of the core state, and using the recently found experimental energies for the first excited states in the single proton nucleus ^{57}Cu [3]:

$$\epsilon(\pi 1f_{5/2})-\epsilon(\pi 2p_{3/2})=1.120\ \text{MeV}, \tag{10}$$

$$\epsilon(\pi 2p_{1/2})-\epsilon(\pi 2p_{3/2})=1.830\ \text{MeV}. \tag{11}$$

The results of the calculations for ^{57}Cu are compared with the experimental data in Fig. 2 and in Table II. We notice also that in both nuclei the first three states are far from being pure single particle and have spectroscopic factors $S(2p_{3/2})=0.86$ and 0.86, $S(1f_{5/2})=0.81$ and 0.79, and $S(2p_{1/2})=0.62$ and 0.64 for ^{57}Ni and ^{57}Cu, respectively. This configuration mixing is most probably the major reason for the departure of the experimental beta decay data for ^{57}Cu [2] from the predictions of the pure single-particle model.

In order to obtain the absolute position of the single-particle levels in the potential well, the absolute energy of the $2p_{3/2}$ orbital was fixed from the neutron (proton) separation energy S_n (S_p) in ^{57}Ni (^{57}Cu) [11] with two corrections:

$$\varepsilon(\nu 2p_{3/2})=-S_n(^{57}\text{Ni})+\Delta\varepsilon_n+\delta_{\rm PVC}. \tag{12}$$

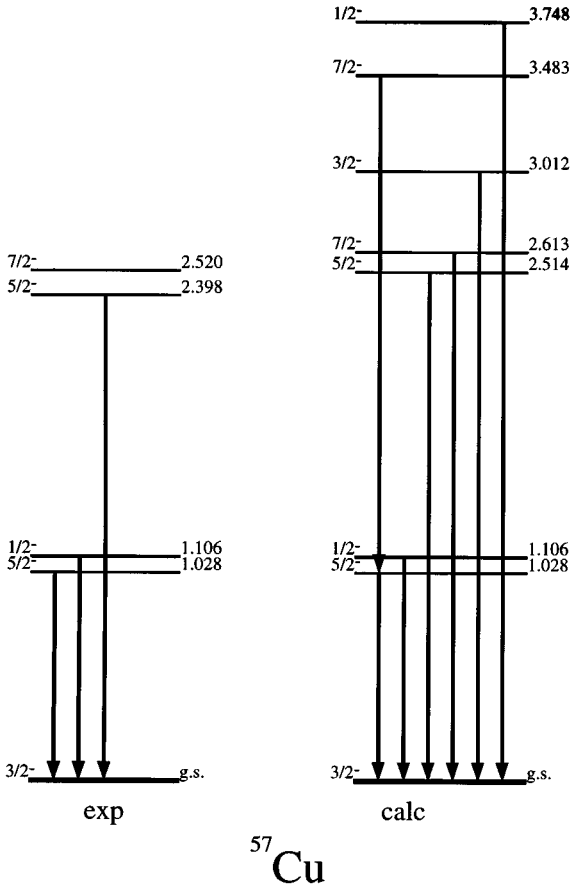

FIG. 2. Same as in Fig. 1, for ^{57}Cu. Data from Ref. [3].

The first correction term $\Delta\varepsilon_n$ takes into account the variation in the single-particle energy when moving from ^{57}Ni, for which the separation energy is measured, to ^{56}Ni for which the single-particle energy is sought. It is calculated following the procedure of Ref. [12]. Corrections of $\Delta\varepsilon_n = -595$ keV and $\Delta\varepsilon_p = -775$ keV were found for neutron and proton states, respectively. The second term accounts for the shift of the ground state energies from the mean-field values due to the contributions from the particle-vibration coupling with an energy $-\delta_{\rm PVC}$ (negative value). From our calculations the ground states were found to be pushed down $\delta_{\rm PVC}$(Ni)=487 keV for ^{57}Ni and $\delta_{\rm PVC}$ (Cu)=483 keV for ^{57}Cu. We adopted a common value $\delta_{\rm PVC}=485$ keV for both nuclei and obtained

$$\varepsilon(\nu 2p_{3/2}) = -10.36 \text{ MeV}, \quad \varepsilon(\pi 2p_{3/2}) = -0.99 \text{ MeV}. \tag{13}$$

A similar correction was included for the $1f_{7/2}$ orbitals. EUM calculations for ^{55}Co considering a $\pi 1f_{7/2}$ hole coupled to the ^{56}Ni core give a fair description of the low-lying states of that nucleus and give a correction $\delta_{\rm PVC} \simeq 290$ keV. We take this correction to be the same for proton and neutron. Subtracting this value from the neutron binding energy of ^{56}Ni, we find the position of the ''bare'' $\nu 1f_{7/2}$ orbital: $\varepsilon(\nu 1f_{7/2}) = -16.93$ MeV.

III. MEAN-FIELD CALCULATIONS

Comparing Eqs. (8) and (10) with (9) and (11), respectively, it appears that the splittings between the proton single-particle states are quite different from those for the neutron. If we denote

$$\Delta\varepsilon_{\pi\nu}(1f_{5/2}) = [\varepsilon(\pi 1f_{5/2}) - \varepsilon(\pi 2p_{3/2})] - [\varepsilon(\nu 1f_{5/2}) - \varepsilon(\nu 2p_{3/2})] \tag{14}$$

and

$$\Delta\varepsilon_{\pi\nu}(2p_{1/2}) = [\varepsilon(\pi 2p_{1/2}) - \varepsilon(\pi 2p_{3/2})] - [\varepsilon(\nu 2p_{1/2}) - \varepsilon(\nu 2p_{3/2})], \tag{15}$$

then we have

$$\Delta\varepsilon_{\pi\nu}(1f_{5/2}) = 290 \text{ keV} \quad \text{and} \quad \Delta\varepsilon_{\pi\nu}(2p_{1/2}) = -50 \text{ keV}. \tag{16}$$

To understand this behavior we have carried out mean-field calculations within the Hartree-Fock approach with commonly used Skyrme-type interactions and by using the local Woods-Saxon potential well.

A. Skyrme Hartree-Fock calculations

In Figs. 3 and 4 we present the results for the neutron and proton single-particle energies of ^{56}Ni obtained from the Skyrme Hartree-Fock (SHF) calculations using the interactions Sk1−Sk6, SkA, SkM* [13], and SkE1−SkE4 [14]. The experimental data and the results obtained using the Woods-Saxon potential, which will be discussed in detail below, are also shown in Figs. 3 and 4. It is seen from Fig. 3 that the SHF results for the single-particle energy splittings $\varepsilon(1f_{5/2}) - \varepsilon(1f_{7/2})$ and $\varepsilon(2p_{1/2}) - \varepsilon(2p_{3/2})$ are in reasonable agreement with the experimental data. However, as seen from Fig. 4, except for the interactions Sk3 and SkE1, the proton and neutron single-particle energy differences $\varepsilon(1f_{5/2}) - \varepsilon(2p_{3/2})$ deviate from the experimental data. Moreover, the SHF results do not reproduce the observed $\Delta\varepsilon_{\pi\nu}(1f_{5/2}) = 290$ keV increase in the proton single-particle energy difference $\varepsilon(1f_{5/2}) - \varepsilon(2p_{3/2})$ compared to that for the neutrons. Clearly, these Skyrme effective interactions would need to be modified to reproduce the spin-orbit splitting (modifying the spin-orbit interaction) and the energy splitting between orbits associated with different values of orbital angular momentum (modifying the effective mass and surface diffuseness of the mean field).

B. Woods-Saxon potential

To investigate the origin of the differences in Eq. (16), we have carried out calculations using a local single-particle potential of the Woods-Saxon form which includes spin-orbit and Coulomb potential:

$$V(r) = V_0\left(1 - 0.67\frac{N-Z}{A}\tau_z\right) f(r) + V_{ls}\vec{s}\cdot\vec{l}\frac{1}{r}\frac{df(\mathrm{r})}{dr} + \frac{1}{2}(1-\tau_z)V_c(r), \tag{17}$$

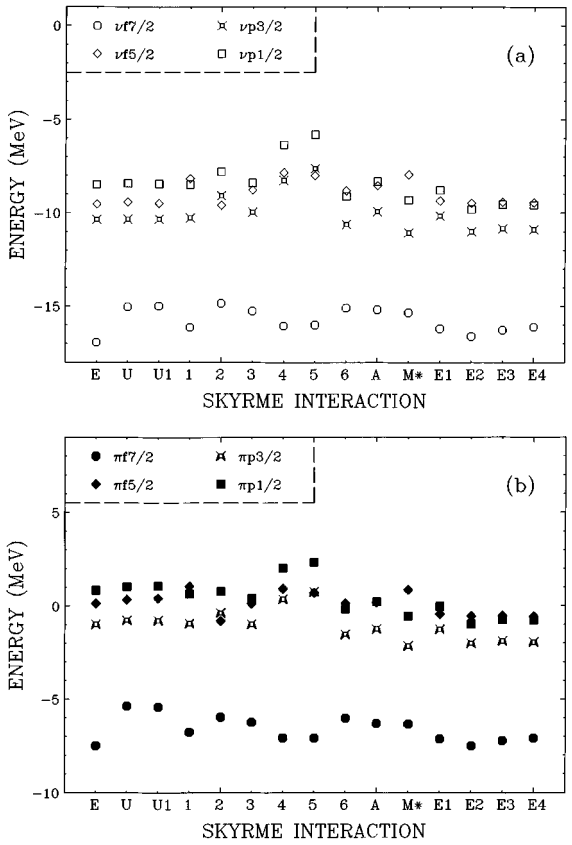

FIG. 3. The single-particle energy levels $1f_{7/2}$, $1f_{5/2}$, $2p_{3/2}$, and $2p_{1/2}$ obtained as a result of Skyrme Hartree-Fock calculations for ^{56}Ni. The interactions Sk1−Sk6, SkA, SkM*, and SkE1−SkE4 are denoted by 1–6, A, M*, $E1$–$E4$ respectively. Also included are the experimental values (denoted by E), the results obtained using the Woods-Saxon potential with Coulomb and spin-orbit terms (denoted by U), and with the contribution of the electromagnetic spin-orbit term ($U1$).

where

$$f(r)=\left[1+\exp\left(\frac{r-R}{a}\right)\right]^{-1}. \tag{18}$$

Here, $R=r_0A^{1/3}$ is the half radius, a is the diffuseness, and V_0 is the depth of the Woods-Saxon potential, V_{ls} is the strength of the spin-orbit potential, and $\tau_z=1$ for a neutron and -1 for a proton. The Coulomb potential is taken to be of the form

$$V_c(r)=\begin{cases}\dfrac{Ze^2}{2R_c}\left[3-\left(\dfrac{r}{R_c}\right)^2\right], & r<R_c,\\ \dfrac{Ze^2}{r}, & r>R_c,\end{cases} \tag{19}$$

which corresponds to an uniform charge distribution with a radius $R_c=(\frac{5}{3})^{1/2}r_c$, where $r_c=\sqrt{\langle r^2\rangle_c}$ is the charge root-mean-square (rms) radius of ^{56}Ni. The charge rms radius r_c of ^{56}Ni is not known. The charge rms radius of ^{58}Ni with two neutrons in the $2p_{3/2}$ orbit was determined by electron scattering [15] to be 3.76 ± 0.02 fm. It is also known [15] that

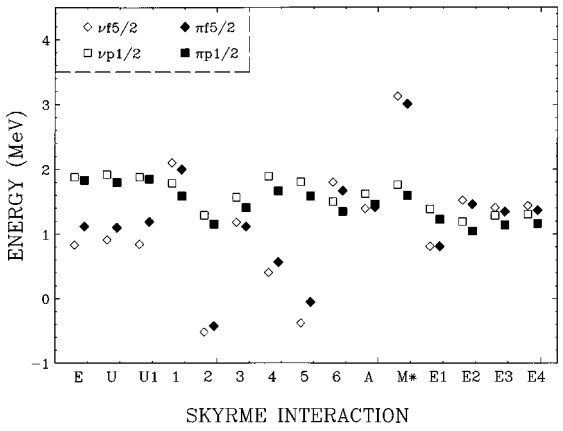

FIG. 4. The splittings of the single-particle energy levels $\varepsilon(1f_{5/2})-\varepsilon(2p_{3/2})$ and $\varepsilon(2p_{1/2})-\varepsilon(2p_{3/2})$ found from Skyrme Hartree-Fock calculations for ^{56}Ni. Notation is the same as in Fig. 3.

r_c of ^{56}Fe with two neutrons in the $2p_{3/2}$ single-particle orbit is larger than that of ^{54}Fe by about 0.05 fm. We therefore take $r_c=3.71$ fm for ^{56}Ni, leading to $R_c=4.8$ fm.

The parameters V_0, r_0, a, and V_{ls} in Eqs. (17) and (18) were determined by a fit to the following experimental data: (i) the single-particle energy $\varepsilon(\nu2p_{3/2})=-10.36$ MeV, (ii) the neutron spin orbit splitting $\varepsilon(\nu2p_{1/2})-\varepsilon(\nu2p_{3/2})=1.88$ MeV, (iii) the neutron single-particle energy difference $\varepsilon(\nu1f_{5/2})-\varepsilon(\nu2p_{3/2})=0.83$ MeV, and (iv) the point proton shell model rms radius $\langle r^2\rangle_{\rm sm}^{1/2}$ in ^{56}Ni deduced from r_c by taking into account the finite size of the proton charge rms radius (0.85 fm) and the effect of the center-of-mass motion:

$$\langle r^2\rangle_{\rm sm}=\langle r^2\rangle_c-(0.85)^2+\frac{1}{A}\frac{3}{2\nu}, \tag{20}$$

where $\nu=m\omega/\hbar$ is the harmonic oscillator size parameter. Using $\hbar\omega=41A^{-1/3}$ MeV, we find $\langle r^2\rangle_{\rm sm}^{1/2}=3.62$ fm.

It is important to point out that in order to reproduce the point proton rms radius of 3.62 fm, we find that $r_0<1.25$ fm. In order to reproduce the experimental values of $\varepsilon(2p_{1/2})-\varepsilon(2p_{3/2})$ and $\varepsilon(1f_{5/2})-\varepsilon(2p_{3/2})$ we find that $a<0.60$ fm. To account properly for the Thomas-Ehrman shift, we determined the direct term of the Coulomb displacement energy as the difference between the single-particle energies calculated with and without the Coulomb potential. A good fit to the experimental data was obtained by using the values $r_0=1.22$ fm, $a=0.57$ fm, $V_0=-53.7$ MeV, and $V_{ls}=18.6$ MeV fm^2. These values are somewhat different from the standard values of $r_0=1.27$ fm, $a=0.67$ fm, $V_0=-51.0$ MeV, and $V_{ls}=17$ MeV fm^2 deduced from a global fit to nuclei along the stability line [5]. The results obtained with the adjusted Woods-Saxon potential are also shown in Figs. 3 and 4 and summarized in Table III.

It is seen from Table III that we have obtained good agreement with the experimental data. However, the Thomas-Ehrman effect increases the value of $\Delta\varepsilon_{\pi\nu}(1f_{5/2})$ by only 0.17 MeV. This is about half of the experimental value of 0.29 MeV [see Eqs. (8) and (10)]. Considering other correction terms (on the level of $\pm1\%$) to the Coulomb dis-

TABLE III. Single-particle energies (MeV) for ^{56}Ni calculated in a Woods-Saxon (WS) potential well with spin-orbit, Coulomb, and electromagnetic spin-orbit interactions [Eqs. (17)–(19)] using the values of $V_0=-53.7$ MeV, $r_0=1.22$ fm, $a=0.57$ fm, $V_{ls}=18.6$ MeV fm,^{2} and $R_c=4.80$ fm.

ε	WS	EMSO	Sum	Expt.
		Neutrons		
$1f_{7/2}$	−15.04	0.045	−14.99	−16.93
$2p_{3/2}$	−10.35	0.014	−10.34	−10.36
$1f_{5/2}$	−9.44	−0.060	−9.50	−9.53
$2p_{1/2}$	−8.43	−0.028	−8.46	−8.48
$1f_{5/2}-1f_{7/2}$	5.60	−0.104	5.50	7.40
$2p_{1/2}-2p_{3/2}$	1.92	−0.042	1.88	1.88
$1f_{5/2}-2p_{3/2}$	0.91	−0.073	0.84	0.83
		Protons		
$1f_{7/2}$	−5.37	−0.053	−5.42	−7.49
$2p_{3/2}$	−0.77	−0.016	−0.79	−0.99
$1f_{5/2}$	0.33	0.070	0.40	0.13
$2p_{1/2}$	1.03	0.031	1.06	0.84
$1f_{5/2}-1f_{7/2}$	5.70	0.123	5.82	7.62
$2p_{1/2}-2p_{3/2}$	1.80	0.047	1.85	1.83
$1f_{5/2}-2p_{3/2}$	1.10	0.086	1.19	1.12

placement energy in mirror nuclei (see Table 6 of Ref. [16]), we find that contributions of the center-of-mass motion, finite size of the nucleon, vacuum polarization, $p-n$ mass difference, and charge symmetry breaking are about the same for the $1f$ and $2p$ single-particle states. However, the sign of the contribution of the electromagnetic spin-orbit (EMSO) term, which is commonly neglected since it is relatively small, is spin and isospin dependent. Since here we are interested in the splitting $\varepsilon(1f_{5/2})-\varepsilon(2p_{3/2})$ for a neutron and a proton, we take a closer look at this correction term.

The electromagnetic spin-orbit interaction $V_{\rm SO}^{\rm EM}$ has the form

$$V_{\rm SO}^{\rm EM}=\frac{\hbar^2}{(2mc)^2}[(g_p-1)(1-\tau_z)+g_n(1+\tau_z)]\vec{s}\cdot\vec{l}\frac{1}{r}\frac{dV_c}{dr}, \tag{21}$$

where V_c is the Coulomb potential from Eq. (15) and $g_p=5.5855$, $g_n=-3.8256$, and $\hbar^2/(2mc)^2=0.0159$ fm^2. Using Eq. (21) in the first order perturbation approximation, we obtained the contribution of the EMSO interaction to the single-particle energies. The results are shown in Table III. We note that taking into account that $R_c>r_c$, the contribution of $V_{\rm SO}^{\rm EM}$ to the single-particle energy can be well approximated by

$$\langle V_{\rm SO}^{\rm EM}\rangle=-(0.0121-0.1337\tau_z)\vec{s}\cdot\vec{l}\frac{Z}{R_c^3}. \tag{22}$$

The values obtained from this approximation, Eq. (22), nicely agree with those in Table III.

As seen from Table III, we have obtained a good agreement between theory and experiment. The contributions of the EMSO interaction to the single-particle energies are about ± 50 keV which affects the spin-orbit splitting by about 100 keV because, unlike the contributions of the spin-orbit interaction associated with the strong interaction, the contributions of the EMSO interaction for proton and neutron single-particle states have opposite signs [see Eq. (21)]. Therefore, it is important to take into account the effect of the EMSO interaction when comparing the single-particle energy spectra of a neutron to those of a proton. In the specific case of the $\varepsilon(1f_{5/2})-\varepsilon(2p_{3/2})$ difference, the EMSO interaction effect increases the value of $\Delta\varepsilon_{\pi\nu}(1f_{5/2})$ by 0.16 MeV. This contribution is as large as the Thomas-Ehrman effect (0.17 MeV). For the $\varepsilon(2p_{1/2})-\varepsilon(2p_{3/2})$ splitting, the Thomas-Ehrman effect decreases $\Delta\varepsilon_{\pi\nu}(2p_{1/2})$ by about 0.105 MeV and the EMSO interaction increases it by 0.090 MeV with a net effect of a decrease by 0.015 MeV. We note that due to the EMSO interaction and the Thomas-Ehrman effect, the $\varepsilon(1f_{5/2})-\varepsilon(1f_{7/2})$ splitting for the proton increases by 0.33 MeV, compared to that for the neutron.

IV. SUMMARY AND CONCLUSIONS

We have considered the low-lying energy levels of the $A=57$ mirror nuclei within the extended unified model, taking into account vibrational core excitations up to three quadrupole phonons and two octupole phonons. Using this model we obtained a good description of the available experimental data on the magnetic moment of the ground state of ^{57}Ni, the excitation energies of the low-lying levels, their lifetimes, B(GT) values, and decay pattern.

We have also extracted from our model calculation the ''bare'' single-particle energies of the $1f_{5/2}$ and the $2p_{1/2}$ proton and neutron single-particle states. These single-particle excitation energies are quite different from the observed excitation energies of the corresponding $5/2_1^-$ and $1/2_1^-$ states in $A=57$ nuclei. Moreover, we find significant differences between the neutron and the proton ''bare'' single-particle excitation energies, with values of $\Delta\varepsilon_{\pi\nu}(1f_{5/2})=290$ keV and $\Delta\varepsilon_{\pi\nu}(2p_{1/2})=-50$ keV. To understand this behavior, we carried out Hartree-Fock calculations with various commonly used Skyrme type effective interactions. We found that although these Skyrme interactions reproduce the gross structure of the single-particle energies, a refinement of these interactions is needed to obtain good overall agreement, considering in particular the spin-orbit term, the effective mass, and the diffuseness of the equivalent local potential.

To investigate further the origin for the shifts in the single-particle energies of the proton compared to those of the neutron, we carried out calculations using a local Woods-Saxon potential well with spin-orbit and Coulomb potential. The parameters of this single-particle potential were adjusted to reproduce the data in ^{56}Ni. Considering possible corrections to Coulomb displacement energies [16], we find that in order to reproduce the differences between the neutron and the proton single-particle excitation energies, it is important to take into account the contributions of the Thomas-Ehrman effect and the electromagnetic spin-orbit interaction. We obtained very good agreement with the data when we included

both of these contributions. An important conclusion of our investigation is that although the contribution of the EMSO term to the single-particle energy is small, about 50 keV, its contribution is spin and isospin dependent. Therefore, the effect of the EMSO term on the difference between the neutron and proton single-particle excitation energies is comparable in magnitude with that associated with the well-known Thomas-Ehrman effect.

ACKNOWLEDGMENTS

One of the authors (S.S.) thanks the Niels Bohr Institute for the kind hospitality. This work was partially supported by the U.S. National Science Foundation (NSF) under Grant No. PHY-9413872, the U.S. Department of Energy under Grant No. DE-FG03-93ER40773, and by the Robert A. Welch Foundation.

[1] M. R. Bhat, Nucl. Data Sheets **67**, 195 (1992).
[2] D. Semon, M. C. Allen, H. Dejbakhsh, C. A. Gagliardi, S. A. Hale, J. Jiang, L. Trache, R. E. Tribble, S. J. Yennello, H. M. Xu, and X. G. Zhou, Phys. Rev. C **53**, 96 (1996).
[3] X. G. Zhou, H. Dejbakhsh, C. A. Gagliardi, J. Jiang, L. Trache, and R. E. Tribble, Phys. Rev. C **53**, 982 (1996).
[4] L. Trache, K. Heyde, and P. von Brentano, Nucl. Phys. **A554**, 118 (1993).
[5] A. Bohr and B. Mottelson, *Nuclear Structure* (Benjamin, Reading, MA, 1969), Vols. 1 and 2.
[6] P. F. Bortignon, R. A. Broglia, D. R. Bes, and R. Liotta, Phys. Rep. **30C**, 305 (1977).
[7] K. Heyde, P. van Isacker, M. Waroquier, J. L. Wood, and R. A. Meyer, Phys. Rep. **102C**, 291 (1983).
[8] G. Kraus, P. Egelhof, C. Fischer, H. Geissel, A. Himmler, F. Nickel, G. Münzenberg, W. Schwab, A. Weiss, J. Friese, A. Gillitzer, H. J. Körner, M. Peter, W. F. Henning, J. P. Schiffer, J. V. Kratz, L. Chulkov, M. Golovkov, A. Ogloblin, and B. A. Brown, Phys. Rev. Lett. **73**, 1773 (1994).
[9] A. M. Oros, L. Trache, P. von Brentano, K. Heyde, and G. Graw, Phys. Scr. **T56**, 292 (1995).
[10] L. Trache, A. Clauberg, C. Wesselborg, P. von Brentano, J. Wrzesinski, R. Broda, A. Berinde, and V. E. Iacob, Phys. Rev. C **40**, 1006 (1989).
[11] G. Audi and A. H. Wapstra, Nucl. Phys. **A565**, 66 (1993).
[12] K. Heyde, J. Jolie, J. Moreau, J. Ryckebusch, and M. Waroquier, Phys. Lett. B **176**, 255 (1986).
[13] J. Friedrich and P.-G. Reinhard, Phys. Rev. C **33**, 335 (1986).
[14] K. Heyde, *The Nuclear Shell Model* (Springer-Verlag, Berlin, 1990), Chap. 8.
[15] H. de Vries, C. W. de Jager, and C. de Vries, At. Data Nucl. Data Tables **36**, 495 (1987).
[16] S. Shlomo, Rep. Prog. Phys. **41**, 957 (1978).